THE JOURNAL OF PHYSICAL CHEMISTRY C

pubs.acs.org/JPCC Article

Nanoparticle-Enhanced Plasma Discharge Using Nanosecond High-Voltage Pulses

Bofan Zhao, Indu Aravind, Sisi Yang, Zhi Cai, Yu Wang, Ruoxi Li, Sriram Subramanian, Patrick Ford, Daniel R. Singleton, Martin A. Gundersen, and Stephen B. Cronin*

Cite This: https://dx.doi.org/10.1021/acs.jpcc.9b12054 Read Online

ACCESS | Metrics & More | Article Recommendations | Supporting Information

ABSTRACT: By discharging nanosecond high-voltage (5 kV) pulses across an insulating substrate containing Au, Pt, or Cu nanoparticles, a 3 order of magnitude (1000×) enhancement in the generation of plasma can be achieved through local field enhancement on the surface of the nanoparticles. The low-temperature nature of this transient plasma is crucial to maintaining the structural integrity of these delicate nanoparticles. These nanoparticles provide up to a 1000-fold enhancement in the generation of the plasma, which is localized to the surface of the nanoparticles where it is potentially useful (e.g., for catalysis). We performed both time-domain and frequency-domain calculations of the electromagnetic response of the nanoparticles based on high-resolution transmission electron microscope (HRTEM) images, which show local field enhancement of the nanosecond high-voltage pulse on the order of 3×. Since the plasma initiation depends exponentially on the peak electric field strength, this 3-fold increase in the local electric field can result in a several orders of magnitude increases in the generation of plasma at a given applied external field strength. In order to rule out plasmon-resonance enhancement, which is often associated with small metal nanoparticles, we performed finite difference time domain (FDTD) simulations in the optical frequency domain, which show that the effect of plasmon resonance is negligible for Pt nanoparticles. We therefore attribute the nanoparticle-based enhancement to the generation of plasma (an electrostatic effect) rather than enhanced coupling of light from the near field to the far field via the plasmon resonance phenomenon (an optical effect).

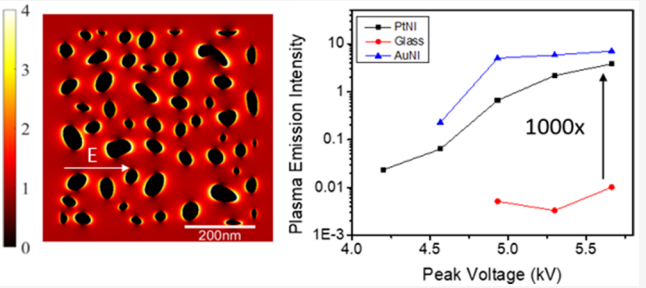

INTRODUCTION

Local electric field enhancement of electron emission (i.e., field emission) has been achieved using nanostructures in which the DC fields are enhanced around a nanoscale sharp feature. For example, carbon nanotubes have been used to produce low-field electron emission with an onset field of as low as 0.8 V/μm following the Fowler−Nordheim equation, which is estimated to be enhanced by 8000-fold with respect to the corresponding bulk material.[1−3] Semiconductor nanowire structures have also been utilized to produce low-field electron emitters and/or enhance field emission current densities.[4−6] Baby et al. reported the effect of metal nanoparticle decoration on the electron field emission property of graphene sheets, in which the nanoparticles provide local field enhancement.[7]

The generation of plasma involves a number of non-deterministic and stochastic processes and is usually initiated by electron emission, followed by acceleration and then ionization of gas molecules.[8] In 1962, Neugebauer and Webb reported that electron conduction on ultrathin metal films deviates from ohmic behavior at high electric fields.[9] Electron emission from discontinuous island metal films was believed to be the reason for this deviation, and typically, this emission is localized in discrete tiny regions referred to as "emission centers". Electron emission from these emission centers has been thoroughly researched in the last century with two main emission mechanisms proposed. In 1972, Dittmer attributed this type of electron emission to standard electric field emission from small islands.[10] However, later works proposed that hot electrons, generated in these mean-free-path-sized nanoparticles, further enhanced the field emission from these nanoislands compared to their bulk counterpart materials.[11−14] In our proposed mechanism, after electrons are emitted outside metal nanoislands, they will be accelerated by the strong electric field and then ionize gaseous molecules in the ambient environment. Once ionized, these gaseous ions are then accelerated in the applied field and in turn ionize other molecules in an avalanche processes that produces a propagating plasma streamer. In our work, we exploit this nanoparticle-based enhancement of electron emission to

Received: December 31, 2019
Revised: February 23, 2020
Published: March 9, 2020

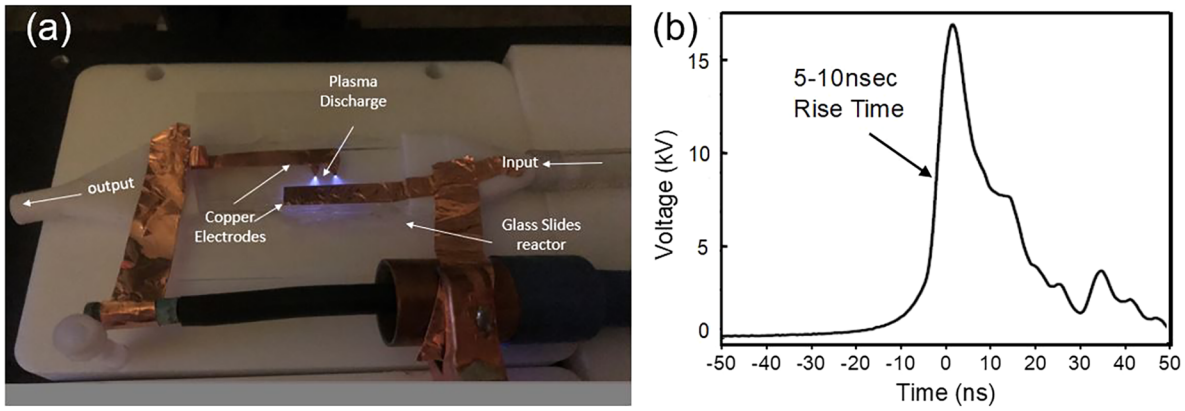

Figure 1. (a) Photograph of the plasma discharge across a 5 mm gap on a glass slide and (b) typical output characteristics of a nanosecond high-voltage pulse generator.

initiate plasma formation at lower applied potentials. Because of the inherent incompatibilities of high voltages typically used to produce plasma discharges (~10 kV) and the small length scales of nanoparticles (~10 nm), nanoparticle enhancement of plasma formation has not yet been demonstrated. Also, physical bombardment by highly energetic ions in the plasma often results in the rapid sputtering and ablation of nanoparticle material, thus making nanoparticles further incompatible with plasma-based processes.[15]

METHODS

In the work presented here, we utilize nanosecond high-voltage pulses to provide a cold plasma, which is far more gentle to the metal nanoparticles than a conventional RF plasma. In order to explore the effects of local field enhancement, we monitor the onset of light emission produced by an argon plasma discharge as a function of peak pulse voltage both with and without nanoparticles. Electrostatics, electrodynamics, and simulations are performed on the nanoparticles based on high-resolution transmission electron microscope (HRTEM) images in order to provide a detailed microscopic picture of the field enhancement process.

We use a 5−10 ns, high-voltage pulse generator (SSPG-20X, Transient Plasma Systems, Inc.) to produce a plasma discharge across two parallel copper electrodes on a glass slide separated by approximately 5 mm, as shown in Figure 1a. The plasma discharge can be seen here in this image as purple light.[16−19] Further details of the experimental setup are given in the Supporting Information document. A typical waveform of the pulse characteristics is plotted in Figure 1b and exhibits a 5−10 ns rise time. Once the streamer is formed, the electric field collapses before a significant amount of current can flow, and as a result, very little power is drawn in the creation of this plasma. Here, the electrons get accelerated to extremely high kinetic energies, initiating a plasma discharge, while the ions in the plasma remain close to room temperature.

The electric field distributions of these nanoparticle films at optical frequencies are calculated using the finite difference time domain (FDTD) method using the Lumerical FDTD-solution software package. Here, an HRTEM image was imported to define the geometry of these nanoparticles in the simulations. Simulations were performed with a mesh size of 1 nm. A plane wave was incident normal to the nanoparticle film. Periodic boundary conditions were applied at the in-plane boundaries, and perfectly matched layer (PML) boundary conditions were applied at the out-of-plane boundaries of the nanoparticle film. Reflected and transmitted powers were measured using power monitors placed behind the source and after the structure, respectively. A 2D field monitor was placed in the plane of the film to record the electric field intensity profile.

RESULTS AND DISCUSSION

Figure 2a shows plasma emission spectra taken in argon (738 nm line) with and without Au nanoparticles with 4.9 kV

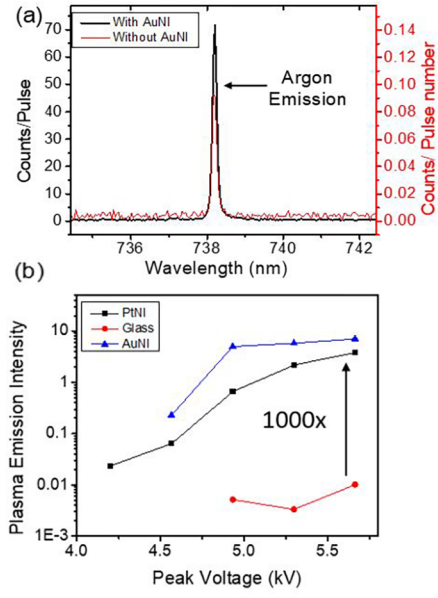

Figure 2. (a) Plasma emission spectra and (b) log−linear plot of the peak area per pulse with and without Au and Pt nanoislands for the 738 nm emission line of Ar.

nanosecond pulses. While the center frequency and line shape of these spectra are nearly identical, the spectrum with nanoparticles is 1000 times more intense than the spectrum taken without nanoparticles. Figure 2b shows the integrated peak intensities plotted as a function of pulse voltage on a log−linear scale with and without both Au and Pt nanoparticles. As mentioned above, the low-temperature nature of this transient plasma is crucial to maintaining the structural integrity of these delicate nanoparticles. We have also seen a similar enhance-

https://dx.doi.org/10.1021/acs.jpcc.9b12054
J. Phys. Chem. C XXXX, XXX, XXX−XXX

ment with Cu nanoparticles, as shown in Figure S1 of the Supporting Information document. The argon plasma exhibits many peaks in the 700−800 nm range, all of which show a similar enhancement.

We deposit nanoparticles using the electron beam evaporation of metals (Pt, Au, and Cu) with nominal thicknesses of 5−10 nm, which are not thick enough to form continuous films and instead create island-like structures.[20−22] Figure 3a shows an HRTEM image of Pt nanoparticles with a 5 nm nominal thickness deposited in this way. In order to understand the role of the electrostatic response of the nanoparticles in the enhancement of plasma generation, we performed quasistatic electromagnetic calculations in which the electric field is changing very slowly and there is no magnetic induction using the AC/DC module in the COMSOL Multiphysics solutions package. Further details of the COMSOL simulation are given in the Supporting Information. Here, we assign floating boundary conditions for the nanoparticles and use an extremely fine physics-optimized mesh on the system, which is essential for accurately treating the short length scales over which fields decay at the nanoparticle surfaces. Figure 3b shows the electric field enhancement observed on Pt nanoparticles in response to the applied DC voltage. Here, we observe a local field enhancement on the order of 3× on surfaces of the nanoparticles. Similar results are observed with Au and Cu nanoparticles. Since the plasma is initiated by the field emission of electrons, which depends exponentially on the electric field, this 3-fold increase in the local electric field can produce a several orders of magnitude increase in the plasma generation, as observed in Figure 2.

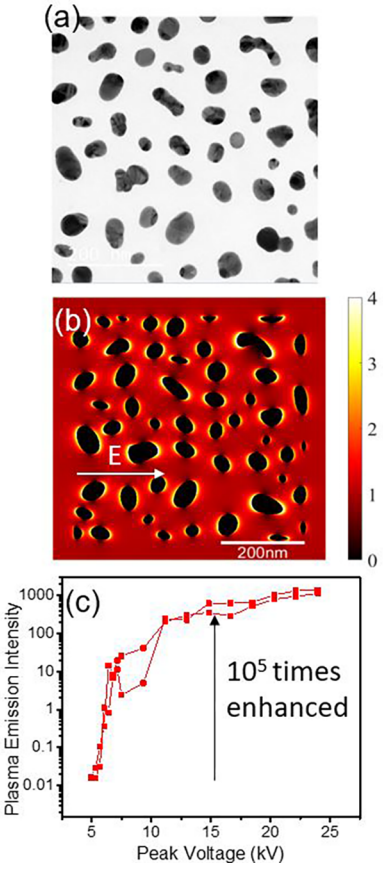

Figure 3. (a) HRTEM image of Pt nanoparticles and (b) quasistatic simulations of the relative electric field enhancement produced by the Pt nanoparticles. (c) Emission intensity on samples with glass only at a different applied voltage.

Metal nanoparticles have been used in the optical frequency domain to enhance Raman scattering for several decades through the surface-enhanced Raman scattering (SERS) phenomenon, which can provide single-molecule sensitivity and an 8−10 orders of magnitude enhancement.[23,24] In order to rule out the possible effects of plasmon-resonance enhancement, often associated with small metal nanoparticles, we performed extensive finite difference time domain (FDTD) simulations in the optical frequency domain (Figure 4).[22,25−31]

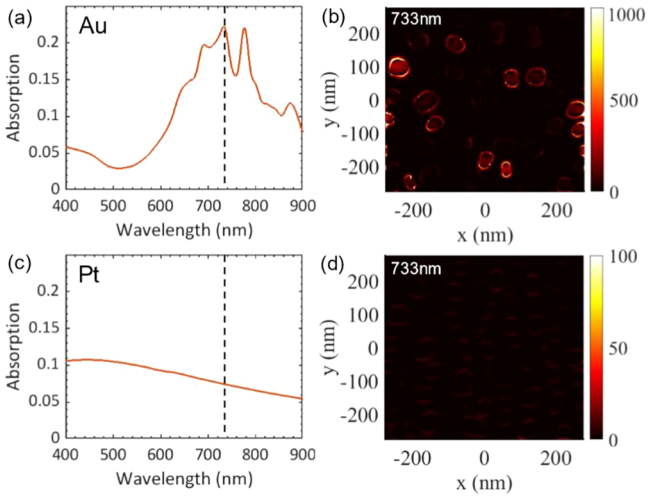

Figure 4. Spectra and electric field intensity distributions of (a, b) Au and (c, d) Pt nanoparticles calculated using the FDTD method.

Figure 4a,b shows the absorption spectrum of an array of Au nanoparticles and a corresponding electric field intensity (i.e., $|E^2|$) distribution at the resonance wavelength of 733 nm. Here, we see localized bright spots (or hot spots) on the surface of the nanoparticles due to the plasmon resonance effect.[22,23] Figure 4c,d show the absorption spectrum of an array of Pt nanoparticles and the corresponding electric field intensity distribution at a wavelength of 733 nm, which shows that the plasmonic effect for Pt nanoparticles is negligible. That is, for nonplasmonic metals such as Pt, there is essentially no enhancement in the local fields at optical frequencies. Since both Pt and Au nanoparticles produce comparable (~1000×) enhancements in the plasma emission spectra (Figure 2), we conclude that the nanoparticle-based enhancement is due to the generation of plasma rather than a coupling of light from the near field to the far field via the plasmon resonance phenomenon.

CONCLUSIONS

We demonstrate a 1000-fold enhancement in the generation of a transient plasma discharged across Pt, Au, and Cu nanoparticles. The main mechanism of enhancement is achieved through local field enhancement at the nanoparticles' surfaces, where it is potentially most useful for applications such as catalysis. This "cold" plasma is relatively gentle and maintains the mechanical integrity of the nanoparticles. On the basis of high-resolution transmission electron microscope (HRTEM) images, we calculate the electrostatic response of

https://dx.doi.org/10.1021/acs.jpcc.9b12054
J. Phys. Chem. C XXXX, XXX, XXX−XXX

the nanoparticles using quasistatic simulations, which predicts a local field enhancement of the nanosecond high-voltage pulse on the order of 3-fold. Because the field emission of electrons is responsible for the initiation of the plasma and depends exponentially on the electric field, this 3-fold increase in the local electric field can produce a several orders of magnitude increase in plasma generation, as observed experimentally. The effect of plasmon-resonance enhancement is ruled out by finite difference time domain (FDTD) simulations performed in the optical frequency domain, which show a negligible enhancement for Pt nanoparticles at optical frequencies. The nanoparticle-based enhancement is therefore attributed to the generation of plasma instead of the plasmonic coupling of light from the far field to the near field.

■ ASSOCIATED CONTENT

Supporting Information

The Supporting Information is available free of charge at https://pubs.acs.org/doi/10.1021/acs.jpcc.9b12054.

Additional data exhibiting a similar enhancement obtained for Cu nanoparticles, detailed figures of our experimental setup, and further details of the COMSOL simulations, including the size dependence of the field enhancement and the distribution of nanoparticle sizes on our samples (PDF)

■ AUTHOR INFORMATION

Corresponding Author

Stephen B. Cronin − *Department of Physics and Astronomy and Ming Hsieh Department of Electrical Engineering, University of Southern California, Los Angeles, California 90089, United States; Transient Plasma Systems, Inc, Torrance, California 90501, United States;* orcid.org/0000-0001-9153-7687; Email: scronin@usc.edu

Authors

Bofan Zhao − *Ming Hsieh Department of Electrical Engineering, University of Southern California, Los Angeles, California 90089, United States*

Indu Aravind − *Department of Physics and Astronomy, University of Southern California, Los Angeles, California 90089, United States*

Sisi Yang − *Department of Physics and Astronomy, University of Southern California, Los Angeles, California 90089, United States;* orcid.org/0000-0003-0352-833X

Zhi Cai − *Mork Family Department of Chemical Engineering and Materials Science, University of Southern California, Los Angeles, California 90089, United States*

Yu Wang − *Mork Family Department of Chemical Engineering and Materials Science, University of Southern California, Los Angeles, California 90089, United States;* orcid.org/0000-0002-0307-1301

Ruoxi Li − *Ming Hsieh Department of Electrical Engineering, University of Southern California, Los Angeles, California 90089, United States*

Sriram Subramanian − *Daniel J. Epstein Department of Industrial & System Engineering, University of Southern California, Los Angeles, California 90089, United States*

Patrick Ford − *Transient Plasma Systems, Inc, Torrance, California 90501, United States*

Daniel R. Singleton − *Transient Plasma Systems, Inc, Torrance, California 90501, United States*

Martin A. Gundersen − *Department of Physics and Astronomy and Ming Hsieh Department of Electrical Engineering, University of Southern California, Los Angeles, California 90089, United States*

Complete contact information is available at: https://pubs.acs.org/10.1021/acs.jpcc.9b12054

Notes

The authors declare no competing financial interest.

■ ACKNOWLEDGMENTS

This research was supported by National Science Foundation (NSF) award nos. CHE-1708581 (R.L.) and CBET-1512505 (I.A.), Air Force Office of Scientific Research (AFOSR) grant no. FA9550-19-1-0115 (B.Z.), Army Research Office (ARO) award no. W911NF-19-1-0257 (Z.C.), and U.S. Department of Energy, Office of Basic Energy Sciences award no. DE-SC0019322 (Y.W.).

■ REFERENCES

(1) Wang, Q. H.; Corrigan, T. D.; Dai, J. Y.; Chang, R. P. H.; Krauss, A. R. Field emission from nanotube bundle emitters at low fields. *Appl. Phys. Lett.* **1997**, *70* (24), 3308−3310.

(2) Bonard, J. M.; Salvetat, J. P.; Stockli, T.; de Heer, W. A.; Forro, L.; Chatelain, A. Field emission from single-wall carbon nanotube films. *Appl. Phys. Lett.* **1998**, *73* (7), 918−920.

(3) Zhu, W.; Bower, C.; Zhou, O.; Kochanski, G.; Jin, S. Large current density from carbon nanotube field emitters. *Appl. Phys. Lett.* **1999**, *75* (6), 873−875.

(4) Zhu, Y. W.; Zhang, H. Z.; Sun, X. C.; Feng, S. Q.; Xu, J.; Zhao, Q.; Xiang, B.; Wang, R. M.; Yu, D. P. Efficient field emission from ZnO nanoneedle arrays. *Appl. Phys. Lett.* **2003**, *83* (1), 144−146.

(5) Lee, C. J.; Lee, T. J.; Lyu, S. C.; Zhang, Y.; Ruh, H.; Lee, H. J. Field emission from well-aligned zinc oxide nanowires grown at low temperature. *Appl. Phys. Lett.* **2002**, *81* (19), 3648−3650.

(6) Fang, X. S.; Bando, Y.; Gautam, U. K.; Ye, C.; Golberg, D. Inorganic semiconductor nanostructures and their field-emission applications. *J. Mater. Chem.* **2008**, *18* (5), 509−522.

(7) Baby, T. T.; Ramaprabhu, S. Effect of metal nanoparticles decoration on electron field emission property of graphene sheets. *Nanoscale* **2011**, *3* (10), 4170−4173.

(8) Piel, A. Stochastic Processes in a Plasma. *Plasma Physics*; Springer: Berlin, 2010; pp 73−106.

(9) Neugebauer, C. A.; Webb, M. B. Electrical Conduction Mechanism in Ultrathin, Evaporated Metal Films. *J. Appl. Phys.* **1962**, *33* (1), 74−82.

(10) Dittmer, G. Electrical conduction and electron emission of discontinuous thin films. *Thin Solid Films* **1972**, *9* (3), 317−328.

(11) Borziak, P. G.; Kulyupin, Y. A.; Nepijko, S. A.; Shamonya, V. G. Electrical conductivity and electron emission from discontinuous metal films of homogeneous structure. *Thin Solid Films* **1981**, *76* (4), 359−378.

(12) Borziak, P. G.; Kulyupin, Y. A. Investigations of discontinuous metal films in the U.S.S.R. *Thin Solid Films* **1977**, *44* (1), 1−19.

(13) Borziak, P.; Kulyupin, Y.; Tomchuk, P. Electron processes in discontinuous metal films. *Thin Solid Films* **1975**, *30* (1), 47−53.

(14) Fedorovich, R. D.; Naumovets, A. G.; Tomchuk, P. M. Electron and light emission from island metal films and generation of hot electrons in nanoparticles. *Phys. Rep.* **2000**, *328*, 73−179.

(15) Minami, T. Transparent conducting oxide semiconductors for transparent electrodes. *Semicond. Sci. Technol.* **2005**, *20* (4), S35−S44.

(16) Saber, I.; Bartnik, A.; Skrzeczanowski, W.; Wachulak, P.; Jarocki, R.; Fiedorowicz, H.; Limpouch, J. Experimental and theoretical study on emission spectra of a nitrogen photoionized plasma induced by intense EUV pulses. *EPJ Web Conf.* **2018**, *167*, 03006.

(17) Zhang, Q. Y.; Shi, D. Q.; Xu, W.; Miao, C. Y.; Ma, C. Y.; Ren, C. S.; Zhang, C.; Yi, Z. Determination of vibrational and rotational temperatures in highly constricted nitrogen plasmas by fitting the second positive system of N_2 molecules. *AIP Adv.* **2015**, *5* (5), 057158.
(18) Martin, W. C.; Sansonetti, J. E. *Basic Atomic Spectroscopic Data*; NIST, accessed Nov 1, 2019; No. 108.
(19) Saloman, E. B. Energy Levels and Observed Spectral Lines of Ionized Argon, Ar II through Ar XVIII. *J. Phys. Chem. Ref. Data* **2010**, *39* (3), 033101.
(20) Kumar, R.; Zhou, H.; Cronin, S. B. Surface-enhanced Raman spectroscopy and correlated scanning electron microscopy of individual carbon nanotubes. *Appl. Phys. Lett.* **2007**, *91*, 223105.
(21) Kneipp, K.; Kneipp, H.; Corio, P.; Brown, S. D. M.; Shafer, K.; Motz, J.; Perelman, L. T.; Hanlon, E. B.; Marucci, A.; Dresselhaus, G.; et al. Surface-enhanced and normal Stokes and anti-Stokes Raman spectroscopy of single-walled carbon nanotubes. *Phys. Rev. Lett.* **2000**, *84* (15), 3470−3473.
(22) Liu, Z.; Hou, W.; Pavaskar, P.; Aykol, M.; Cronin, S. Plasmon Resonant Enhancement of Photocatalytic Water Splitting Under Visible Illumination. *Nano Lett.* **2011**, *11*, 1111.
(23) Dieringer, J. A.; Lettan, R. B.; Scheidt, K. A.; Van Duyne, R. P. A frequency domain existence proof of single-molecule surface-enhanced Raman Spectroscopy. *J. Am. Chem. Soc.* **2007**, *129* (51), 16249−16256.
(24) Kneipp, K.; Wang, Y.; Kneipp, H.; Perelman, L. T.; Itzkan, I.; Dasari, R.; Feld, M. S. Single molecule detection using surface-enhanced Raman scattering (SERS). *Phys. Rev. Lett.* **1997**, *78* (9), 1667−1670.
(25) Chen, J. H.; Bailey, C. S.; Hong, Y. L.; Wang, L.; Cai, Z.; Shen, L.; Hou, B. Y.; Wang, Y.; Shi, H. T.; Sambur, J.; et al. Plasmon-Resonant Enhancement of Photocatalysis on Monolayer WSe2. *ACS Photonics* **2019**, *6* (3), 787−792.
(26) Wang, Y.; Shen, L.; Wang, Y.; Hou, B.; Gibson, G. N.; Poudel, N.; Chen, J.; Shi, H.; Guignon, E.; Cady, N. C.; et al. Hot electron-driven photocatalysis and transient absorption spectroscopy in plasmon resonant grating structures. *Faraday Discuss.* **2019**, *214* (0), 325−339.
(27) Wang, Y.; Shen, L.; Wang, Y.; Hou, B.; Gibson, G. N.; Poudel, N.; Chen, J.; Shi, H.; Guignon, E.; Cady, N. C.; et al. Hot Electron-driven Photocatalysis and Transient Absorption Spectroscopy in Plasmon Resonant Grating Structures. *Faraday Discuss.* **2019**, *214*, 325.
(28) Qiu, J.; Zeng, G.; Pavaskar, P.; Li, Z.; Cronin, S. B. Plasmon-Enhanced Water Splitting on TiO_2-Passivated GaP Photocatalysts. *Phys. Chem. Chem. Phys.* **2014**, *16*, 3115.
(29) Hou, W.; Cronin, S. A Review of Surface Plasmon Resonance-Enhanced Photocatalysis. *Adv. Funct. Mater.* **2013**, *23*, 1612.
(30) Hou, W.; Liu, Z.; Pavaskar, P.; Hung, W. H.; Cronin, S. B. Plasmonic Enhancement of Photocatalytic Decomposition of Methyl Orange under Visible Light. *J. Catal.* **2011**, *277*, 149.
(31) Hung, W. H.; Aykol, M.; Valley, D.; Hou, W. B.; Cronin, S. B. Plasmon Resonant Enhancement of Carbon Monoxide Catalysis. *Nano Lett.* **2010**, *10* (4), 1314−1318.

https://dx.doi.org/10.1021/acs.jpcc.9b12054
J. Phys. Chem. C XXXX, XXX, XXX−XXX